Supplementary Information

Supplementary Text

Plasmids and yeast strains construction

Plasmids and yeast strains are listed in Tables S2 and S3, respectively. Site-directed mutagenesis was performed by QuikChange mutagenesis (Stratagene), and verified by sequencing. Fragments of *SSK2* (*SSK2*: 1-1695, 1696-3225, 3226-4737) or *SLN1* (*SLN1:* 1063-1371) were amplified by PCR with oligos containing BamH1 and Sal1 restriction sites, and cloned into pGEX-4T-1 or pGEX-6P-1, respectively. The SLN1-3A mutant harbours alanine substitutions of the residues S380, T381 and S451, SSk1-4A mutant of the residues S110, S193, S195 and S351, and the SSK2-8A mutant of the residues S54, S57, S68, S74, S78, T172 and S176. The *HOG1-mCherry-HIS3* locus with its endogenous promoter and terminator (580 and 554 bases, respectively) was amplified by PCR from genomic DNA and ligated into pRSII325 [1] using the XhoI and NotI restriction sites. Lysine 52 and 53 were then mutated to serine and asparagine residues to yield the kinase-inactive Hog1 mutant ($hog1^{KN}$). All constructs were confirmed by the size of fragments on agarose gel and sequencing.

The *hog1KN* (K52S, K53N) *-mCherry-HIS3* strain (yHS202) was constructed by transforming the linearized plasmid (pHS51) in *hog1*Δ strains. *sln1-2A* and *sln1-3A* mutants (yKS22 and 24) were constructed by deleting a small region downstream of the trans-membrane domain (1219-1254) in *ssk1*Δ cells. Mutated versions of the *SLN1L* region (2A: S380A, T381A; 3A: S380A, T381A, S451A) were created by PCR using oligos with appropriate mutations, and introduced in *slnl*Δ strains by homologues

recombination and selection using the URA/5-FOA system. Successful integration of mutations was confirmed by sequencing. *sln1-3A* with its endogenous promoter and terminator (766 and 552 bases, respectively) was amplified by PCR from yKS24 genomic DNA and ligated into a vector containing ScHIS3 and the *TEF* terminator (pBH171) using the NotI and SalI restriction sites. The *TEF* terminator was used as a homologous recombinant region with the *KAN* cassette in the *sln1*Δ*ssk1*Δ background. Ssk1 was then retrieved by crossing to the wild-type W303 cells to construct yHS221. *ssk2-8A* strains were created by deleting the N-terminal part of *SSK2*. The mutant PCR fragment was amplified from pGEX *ssk2-8A* vector, transformed into *ssk2N*Δ*::URA3* strains by homologues recombination and selected by growth on 5-FOA plates. *ssk2-8A* with its endogenous promoter and terminator was amplified by PCR from ySR266 genomic DNA and integrated in *ssk2*Δ in the W303 background to construct yHS218. As a control wild-type Ssk2 TAP tagged was also constructed (yHS222), which behaves like the untagged version in our assay.

Computational model description

We developed an ODE based model including the phosphorelay and the MAPK signaling cascade. All reactions are listed in Table S 4 and are solved assuming mass action kinetics. The MATLAB SimBiology® toolbox was used with the ODE solver (ode15s), and the time scale was adjusted using experimental data for the wild-type condition (Fig 2C). For modeling feedback mechanisms we assumed that Hog1 phosphorylation inactivates Ssk2, and targets phospho-Ssk1-Asp (Ssk1-Asp-p) and phospho-Sln1-Asp (Sln1-Asp-p). Hog1 phosphorylates its targets at amino acid(s) X. When Ssk2 is

phosphorylated at amino acid(s) X by Hog1, Ssk2-X-P fails to bind Ssk1 and can thus not be activated. Likewise Asp_{554}–P on Ssk1 cannot undergo activation through hydrolysis when phosphorylated by Hog1. To simplify our model, the feedback reactions were modeled assuming that the Hog1 phosphorylation results in complete inhibition of its substrate. *In vivo* Hog1 probably dampens the activity of its targets. In the case of Sln1, phosphorylation by Hog1 increases the phosphotransfer rates between Sln1-His576, Sln1-Asp1144, and Ypd1-His64. The phosphotransfer rates kpYpd1FAST and kpAspFAST are five times larger than kpYpd1 and kpAsp (Table S 4). As a result the concentrations of phospho-Ypd1 and phospho-Ssk1 increase, resulting in dampened Hog1 activation. For simplicity and to reduce the number of parameters, we assumed that dephosphorylation happens with a constant rate and no specific phosphatases were defined. The initial values for the simulated reactants were set according to http://yeastgfp.yeastgenome.org/. Proteins concentrations are entered as μM, by considering a cell volume of 40 μm^3 (http://bionumbers.hms.harvard.edu/). The rate constants were adjusted empirically to qualitatively resemble experimental data. This approach works if the model is designed to study relative phenotypes compared to the control experiments but is not suited to learn about absolute values of system's parameters. Consequently, we performed parameter scanning only to evaluate the sensitivity of each feedback loop. For studying the effects of the variations of feedback parameters on the signaling feedback efficiency (SFE), we set all feedback parameters [k1, k_1, k2, kp] (binding, dissociation, release and dephosphorylation rates) to the upper limit value, respectively [0.1667, 0.0167, 0.5, 0.0083]. SFE starts decreasing by increasing the feedback parameters more than this upper limit, which is counterintuitive.

Therefore increasing feedback parameters above the upper limit is excluded from the exploration space. Then to see how SFE reduces by making the feedback weaker, we iteratively decreased the feedback parameters (k1, k_1, k2 and kp) by dividing by 1, 2, 3, 4 and 5.

To assess the sensitivity of the basal level of Hog1PP (phosphorylated Hog1) to the parameters of the model (excluding feedback parameters), we performed a sensitivity analysis and calculated d(Hog1PP (t))/dk, where k is a parameter. All sensitivities are less than one, indicating that Hog1 phosphorylation will not considerably change by altering the parameters. Hog1PP was most sensitive to some parameters (Table S 5) that directly affected its activity including the association rate of Pbs2 and Hog1 and the dephosphorylation rate of Hog1.

Since we are lacking mechanistic understanding of how the presence of glucose is sensed, a simplified model was considered, assuming that the phosphorylation rate of Hog1 is a function of glucose availability. *f*(glucose) in Table S 4 represents the glucose switch whose value exponentially decreases and tends to zero during starvation, but exponentially increases and reaches a constant rate at the end of the starvation time.

Table S 1: Time course of proteins phosphorylation detected by shotgun mass spectrometry in response to salt stress

Protein	Peptide sequence	Phospho-sites	Time after addition of 0.4M NaCl (min)					
			- NaCl	1	5	10	20	45
Ssk1	FASVSP YPK	S193 S195	1.53E-5	2.19E-5	4.29E-5	5.28E-5	4.84E-5	3.00E-5
Ssk2	VASSPIS PGLHST QYFR	S53 S54 S57	5.11E-5	1.43E-4	1.24E-4	1.13E-4	1.05E-4	6.81E-5
	SPNAVY SPGESPL NTVQLF NR	S74 S78	2.96E-5	4.39E-5	6.17E-5	6.20E-5	3.58E-5	2.02E-5
Hog1	IQDPQM TGYVST R	T174 Y176	3.52E-05	9.12E-04	8.10E-04	3.11E-04	1.05E-04	7.05E-05

Phosphorylation of the indicated peptides was monitored by mass-spectrometry in the absence (- NaCl) or at the indicated times (in minutes) after addition of 0.4 M NaCl. The numbers indicate normalized intensities. Note that phosphorylation of the highlighted serine residues (green) was increased upon addition of 0.4M NaCl and declined when cells adapted to the high osmolarity conditions. Moreover, these phosphosites on Ssk1 and Ssk2 were not detected when Hog1 activity was inhibited by addition of the 1-NA-PP1 kinase inhibitor.

Table S 2: List of plasmids used in this study

Plasmid	Insert	Vector	Source/ Reference
pSP54	FPS1	YEp	[2]
pSP55	*fps1Δ1*	YEp	[2]
pFD70	STE11::URA3		[3]
pSP109	p*ADH1*-GAL4DBD-hER-VP16*		[4]
pHS21	p*GAL1-ssk2ΔN*	pYES2	[5]
pMK43	G418-linker_IAA17		[6]
pNHK53	URA3-p*ADH1*-OsTIR1-9myc		[6]
pHS24	p*GAL1-ssk1-D554S*	pRS413	[7]
pHS51	*hog1KN-mCherry-HIS3*	pRSII325	This study
pHS17	*ssk1-4A*-ScHIS3-TEF tr		This study
pHS54	*sln1-3A*-ScHIS3-TEF tr		This study
pHS55	FPS1	pRSII425	This study
pHS56	*fps1Δ1*	pRSII425	This study

* ADGEV plasmid

Table S 3: List of yeast strains used in this study

Strain	Genotype	Source/ Reference
ySP110	*MAT***a**[§] hta2::hta2-CFP hog1::hog1-mCherry-HIS3	[8]
yHS110	*MAT***a**[§] hta2::hta2-CFP hog1::hog1-mCherry-URA3	This study
yHS223	*MAT***a**[§] hta2::hta2-CFP hog1::hog1-mCherry-URA3 Leu2-p*FPS1*-FPS1	This study
yHS224	*MAT***a**[§] hta2::hta2-CFP hog1::hog1-mCherry-URA3 Leu2-p*FPS1-fps1Δ1*	This study
yHS206	*MAT***a**[§] hta2::hta2-CFP hog1::hog1-mCherry-URA3 pbs2::NAT	This study
yHS202	*MAT***a**[§] hta2::hta2-CFP hog1::hog1KN-mCherry-HIS3	This study
yHS187	*MAT***a**[§] hta2::hta2-CFP hog1::hog1-mCherry-HIS3 ste11::URA3	This study
yHS123	*MAT***a**[§] hta2::hta2-CFP hog1::hog1-mCherry-HIS3 ssk1::NAT	This study
yHS140	*MAT***a**[§] hta2::hta2-CFP hog1::hog1-mCherry-HIS3 trp1::TRP1-ADGEV ssk2::kanMX URA3-p*GAL1-ssk2ΔN*	This study
yHS68	*MAT***a**[§] hta2::hta2-CFP hog1::hog1-mCherry-HIS3 ypd1::ypd1-GFP-AID-kanMX	This study
yHS69	*MAT***a**[§] hta2::hta2-CFP hog1::hog1-mCherry-HIS3 ypd1::ypd1-GFP-AID-kanMX ura3:: URA3-p*ADH1*-OsTIR1-9myc	This study
yHS145	*MAT***a**[§] hta2::hta2-CFP hog1::hog1-mCherry-URA3 ssk1::NAT trp1::TRP1-ADGEV HIS3-p*GAL1-ssk*1-*D554S*	This study
yHS130	*MAT***a**[§] hta2::hta2-CFP hog1::hog1-mCherry-URA3 ssk1::*ssk1-4A*-HIS3	This study
yHS218	*MAT***a**[§] hta2::hta2-CFP hog1::hog1-mCherry-URA3 ssk2::*ssk2-8A*-TAP-HIS3	This study
yHS221	*MAT***a**[§] hta2::hta2-CFP hog1::hog1-mCherry-URA3 sln1::*sln1-3A*-HIS3	This study

Strain	Genotype	Source/ Reference
yHS222	*MAT***a**[§] hta2::hta2-CFP hog1::hog1-mCherry-URA3 ssk2::*ssk2*-TAP-HIS3	This study
ySR266	*MAT***a**[†] ssk2::*ssk2-8A*-TAP-HIS3 sho1::kanMX ssk22::LEU2 hog1::*hog1as*	This study
yKS22	*MAT***a**[†] ssk2::*ssk2*-TAP-HIS3 sho1::kanMX ssk22::LEU2 ssk1::NAT hog1::*hog1as* sln1::*sln1-2A*	This study
yKS24	*MAT***a**[†] ssk2::*ssk2*-TAP-HIS3 sho1::kanMX ssk22::LEU2 ssk1::NAT hog1::*hog1as* sln1::*sln1-3A*	This study

§ W303 background

† BY4741 background

Table S 4: List of reactions used in the computational model

Reactions	Kinetic rates*	Values
Phosphorelay		
Sln1-Asp → Sln1-Asp-p	kpAsp	6.6667 s^{-1}
Sln1-Asp-p + Ypd1 → Sln1-Asp + Ypd1-p	kpYpd1	6.6667 $(\mu M.s)^{-1}$
Ssk1-OH + Ypd1-p → Ssk1-Asp-p + Ypd1	kpSsk1	6.6667 $(\mu M.s)^{-1}$
Ssk1-Asp-p → Ssk1-OH	kOH	0.3 s^{-1}
Ssk2 activation/inactivation		
Ssk1-OH + Ssk2 ↔ {activeSsk2}	k_act k_inh	6.6667 $(\mu M.s)^{-1}$ 0.3333 s^{-1}
Pbs2 phosphorylation/dephosphorylation		
{activeSsk2} + Pbs2 ↔ {Ssk2_Pbs2} → {activeSsk2} + Pbs2PP	k1_KKr1st, k_1_KKr1st, k2_KKi1st	5 $(\mu M.s)^{-1}$ 0.5 s^{-1} 7.5 s^{-1}
Pbs2PP → Pbs2	k1_dePhr_KK1	0.01
Hog1 phosphorylation		
Pbs2PP + Hog1 ↔ {Pbs2PP_Hog1} → Pbs2PP + Hog1PP	k1_Kr1st, k_1_Kr1st, f(glucose)†	1.6667 $(\mu M.s)^{-1}$ 0.1667 s^{-1}
Glucose switch		
GluSw = k2_Ki1st [1-H(t-Sw1)(1-$e^{-dec(t-Sw1)}$) + H(t-Sw2)(1-$e^{-asc(t-Sw2)}$)] H is a Heaviside step function; Sw1 and Sw2 correspond to switching times.	k2_Ki1st dec asc	2.5 s^{-1} 0.0667 s^{-1} 0.002 s^{-1}
Hog1 dephosphorylation		
Hog1PP → Hog1	k1_dePhr_K1	0.0333 s^{-1}
Feedback to Sln1		
Sln1-Asp-p + Hog1PP ↔ {Sln1Hog1} → Sln1-Dp-Xp + Hog1PP	k1Sln1fdbk, k_1Sln1fdbk, k2Sln1fdbk	0.1667 $(\mu M.s)^{-1}$ 0.0167 s^{-1} 0.5 s^{-1}

Reactions	Kinetic rates*	Values
Sln1-Dp-Xp + Ypd1 → Sln1-Asp-Xp + Ypd1-p	kpYpd1FAST	33.3333 $(\mu M.s)^{-1}$
Sln1-Asp-Xp → Sln1-Dp-Xp	kpAspFAST	33.3333 s^{-1}
Sln1-Dp-Xp → Sln1-Asp-p	kpXpSln1fdbk	0.0083 s^{-1}
Sln1-Asp-Xp → Sln1-Asp	kpXpSln1fdbk	0.0083 s^{-1}
Feedback to Ssk1		
Ssk1-Asp-p + Hog1PP ↔ {Ssk1Hog1} → Ssk1-Dp-Xp + Hog1PP	k1Ssk1fdbk, k_1Ssk1fdbk, k2Ssk1fdbk	0.1667 $(\mu M.s)^{-1}$ 0.0167 s^{-1} 0.5 s^{-1}
Ssk1-Dp-Xp → Ssk1-Asp-p	kpXpSsk1fdbk	0.0083 s^{-1}
Feedback to Ssk2		
Hog1PP + Ssk2 ↔ {Hog1Ssk2} → Hog1PP + Ssk2-Xp	k1Ssk2fdbk, k_1Ssk2fdbk, k2Ssk2fdbk	0.0556 $(\mu M.s)^{-1}$ 0.0056 s^{-1} 0.1667 s^{-1}
Ssk2-Xp → Ssk2	kpSsk2fdbk	0.0028 s^{-1}
Ypd1 degradation		
Ypd1 ↔ null	k_deg, k_pro	0.3 s^{-1} 0.0003 $\mu M.\ s^{-1}$

*: k1 and k_1 are respectively the forward and reverse kinetic rates in the corresponding reactions.

†: *f*(glucose) is simulating the glucose switch which is defined by GluSw.

Table S 5: Sensitivity analysis for the most sensitive parameters for the model without feedback

Parameter	Sensitivity value	Description
k1_Kr1st	0.57	Association rate of Pbs2 and Hog1
k1_dePhr_K1	-0.59	Dephosphorylation rate of Hog1
k1_KKr1st	0.47	Association rate of Ssk2 and Pbs2
k1_dePhr_KK1	-0.47	Dephosphorylation rate of Pbs2
k-act	0.38	Activation rate of Ssk2
k-inh	-0.38	Inactivation rate of Ssk2
k-OH	0.39	Hydrolysis rate of Asp554 on Ssk1
k-p-Ssk1	-0.27	Phosphorylation rate of Asp554 on Ssk1

References

1. M. K. Chee and S. B. Haase, *G3 (Bethesda)*, 2012, **2**, 515–526.
2. M. Tamas, K. Luyten, F. C. W. Sutherland, A. Hernandez, J. Albertyn, H. Valadi, H. Li, B. A. Prior, S. G. Kilian, J. Ramos, L. Gustafsson, J. M. Thevelein, and S. Hohmann, *Molecular Microbiology*, 1999, **31**, 1087–1104.
3. F. Drogen, S. M. O'Rourke, V. M. Stucke, M. Jaquenoud, A. M. Neiman, and M. Peter, *Curr. Biol.*, 2000, **10**, 630–639.
4. S. Takahashi and P. M. Pryciak, *Curr. Biol.*, 2008, **18**, 1184–1191.
5. F. Posas and H. Saito, *Science*, 1997, **276**, 1702–1705.
6. K. Nishimura, T. Fukagawa, H. Takisawa, T. Kakimoto, and M. Kanemaki, *Nat. Methods*, 2009, **6**, 917–922.
7. T. Horie, K. Tatebayashi, R. Yamada, and H. Saito, *MCB*, 2008, **28**, 5172–5183.
8. S. Pelet, R. Dechant, S. S. Lee, F. van Drogen, and M. Peter, *Integr Biol (Camb)*, 2012, **4**, 1274–1282.

Supplementary Figures

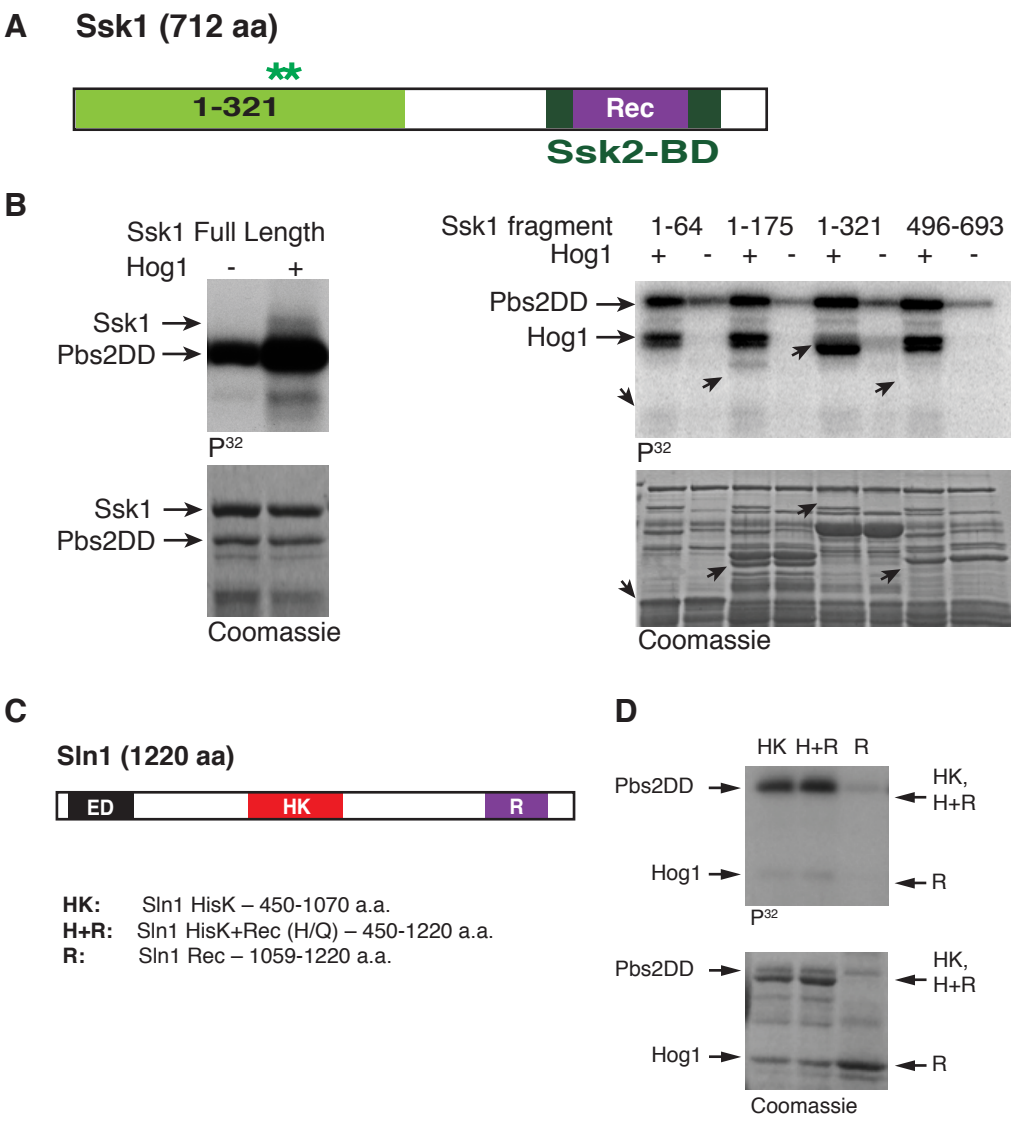

Fig. S 1: Phosphorylation analyses of Ssk1 and Sln1 fragments *in vitro*.

A A schematic diagram of Ssk1 linear amino acid sequence indicating the phosphorylated amino-terminal fragment (light green), the receiver domain (Rec), and Ssk2 binding domain (Ssk2-BD). S193 and S195 (green asterisks) are phosphorylated *in vivo* upon addition of 0.4M NaCl in a Hog1-dependent manner.

B Ssk1 is weakly phosphorylated by Hog1 in its N-terminal region (1-321) *in vitro*. Purified full-length (left panel) or the indicated fragments of Ssk1 (right panel, arrows) were incubated with pre-activated Hog1 (see Materials and Methods) in the presence of ^{32}P-γ-ATP. The upper panels show autoradiographs to visualize phosphorylation of the different proteins, while Coomassie staining (lower panels) controls protein amounts.

C Schematic diagram highlighting the domain structure of Sln1. ED: extracellular domain, HK: Histidine Kinase, R: Receiver domain.

D The HK (Histidine Kinase) and R (Receiver) domains of Sln1 are not phosphorylated *in vitro*. Purified fragments of Sln1 were incubated with pre-activated Hog1 as described in panel B.

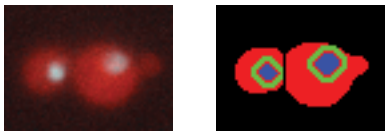

Fig. S 2: Image segmentation and quantification of Hog1 translocation
The left image shows a merged picture of cells expressing Hta2-CFP (cyan) and Hog1-mCherry (red). In the right image, segmentation by the image analysis routine using the RFP and CFP signals shows the cytosol (red) and the nucleus (blue). The green region around the nucleus (rim) is defined as 1 pixel away from the nucleus object with the width of 2 pixels.

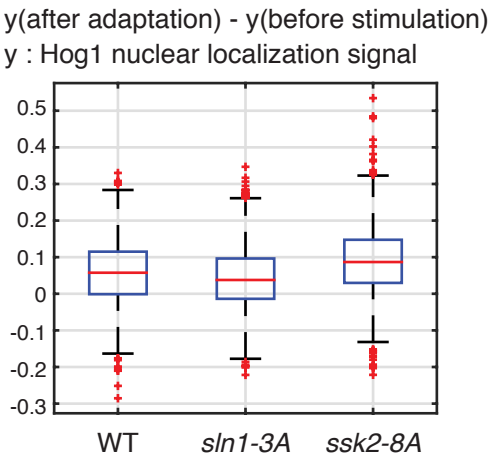

Fig. S 3: Box plot of final minus initial Hog1 nuclear enrichment for WT, *sln1-3A* and *ssk2-8A* cells obtained from data shown in Fig. 1G.

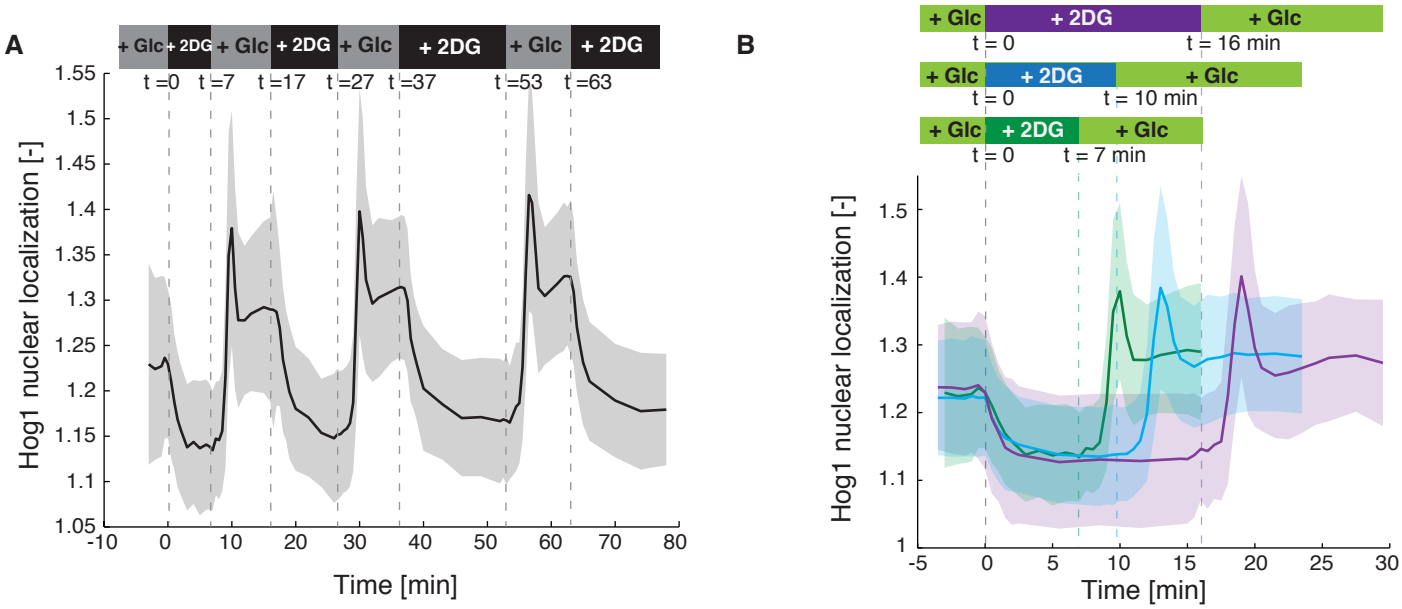

Fig. S 4: The overshoot peak slightly increases by increasing the starvation duration.

A Hog1 nuclear localization over time in wild-type (WT, n=127) cells treated sequentially with 2% 2-deoxy-d-glucose (2DG) and glucose. Cells expressing Hog1-mCherry were added to the microfluidic chamber, the media was exchanged as indicated (gray bar). Note that the maximum value of the Hog1 nuclear enrichment following switching to glucose increases by increasing the duration of starvation.

B Hog1 nuclear localization in wild-type (WT) cells in response to varying starvation periods. Cells expressing Hog1-mCherry were added to the microfluidic chamber, were starved for 7, 10 and 16 minutes (green, blue and purple curves, n=127, 336 and 126 and respectively). Note that the overshoot amplitude increases slightly by extending the starvation duration consistent with the fact that the Hog1 dependent inhibitory signal becomes larger by turning Hog1 activity off for a longer time interval. (A and B) The shaded areas show the standard deviation of the averaged data from indicated number of cells.

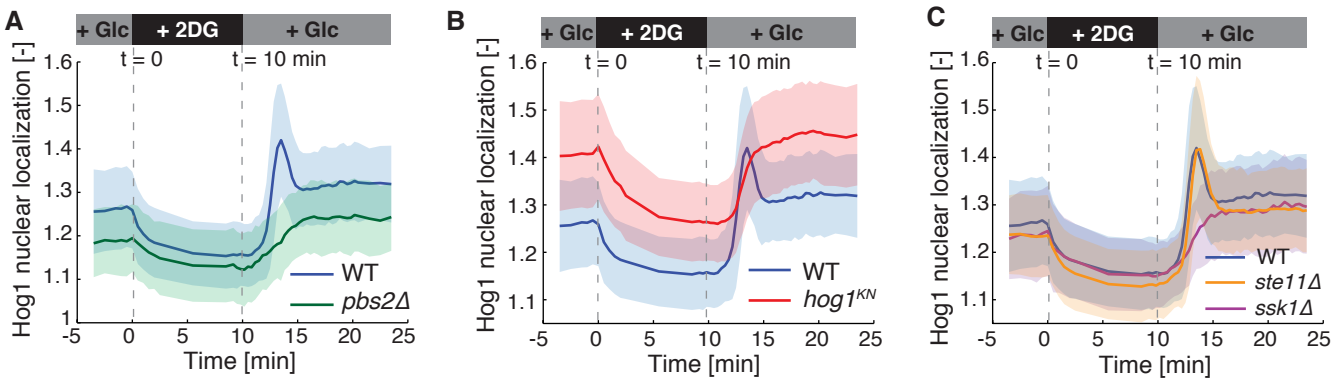

Fig. S5: Complete profile of Hog1 nuclear localization in response to glucose deprivation and re-addition for the data shown in Fig. 2 C-E.

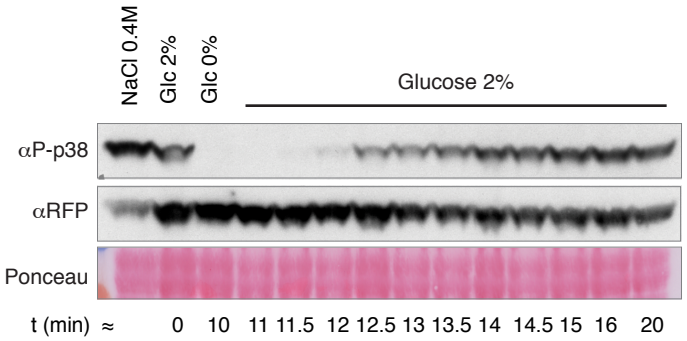

Fig. S 6: Phosphorylation of kinase-inactive *hog1^{KN}* is diminished by glucose deprivation and gradually increased after re-adding glucose.

Cells expressing *Hog1^{KN}*-mCherry were grown in SC-full medium containing 2% glucose (Glc 2%, time 0), washed and resuspended in S-full medium lacking glucose (Glc 0%) for 10 minutes (t = 10 min). Glucose (2%) was then added and aliquots were taken at the times indicated. Cells were fixed with 10% TCA, and Hog1 phosphorylation was monitored by western blotting with antibodies specific for phospho-p38, which cross-react with yeast phospho-Hog1.

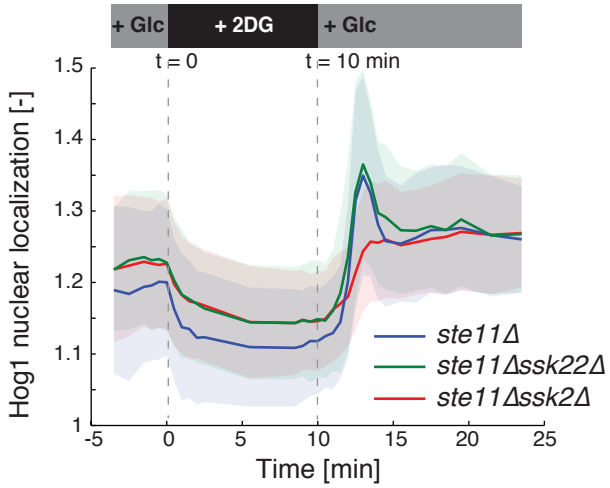

Fig. S 7: Overshoot of nuclear Hog1 is independent of the MAPKKK Ssk22.

Hog1 nuclear localization was quantified over time during the glucose-switch (grey bar) in *ste11Δ* (blue, n=212), *ste11Δssk22Δ* (green, n=158) and *ste11Δssk2Δ* (red, n=228) cells. The shaded areas show the standard deviation of the averaged data from indicated number of cells.

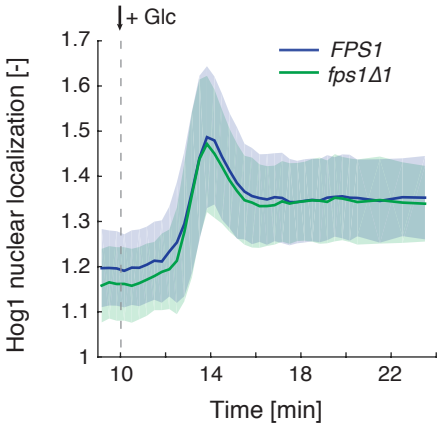

Fig. S 8: The overshoot of Hog1 activity is independent of cytoplasmic glycerol accumulation. Hog1 nuclear localization was quantified upon addition of 2% glucose to the starvation medium containing 2% 2-DG in cells carrying wild-type Fps1 (FPS1, blue curve, n=248) or the constitutively-open glycerol channel mutant *fps1Δ1* (green curve, n=207) expressed from a 2*μ* plasmid. The shaded areas show the standard deviation of the averaged data from indicated number of cells.

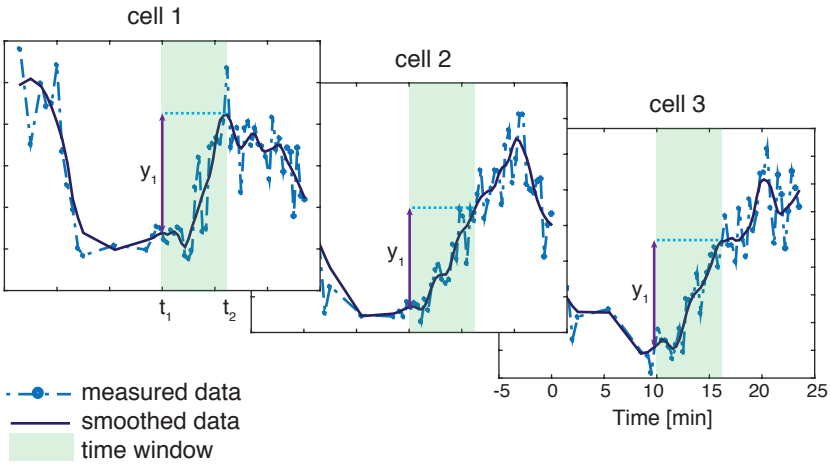

Fig. S 9: Single-cell traces from *ssk1Δ* cells where most of the cells have SFE=0. Note that since the maximum reaches at the end of the time window, y_2 (as described in the Material and methods) and consequently the SFE is zero.

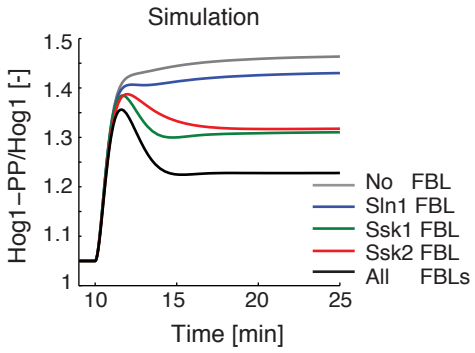

Fig. S 10: Simulation results for Hog1 activity with all feedback loops (black, all FBLs), without feedback (gray), with a single feedback loop acting only on Ssk2 (red), Ssk1 (green) or Sln1 (blue). The ratio between phosphorylated Hog1 (Hog1-PP) and total Hog1 is plotted versus time (min). The glucose starvation condition is simulated in the model for 10 min and the normalized Hog1 activity is followed upon implementation of the glucose switch in the model (see computational model description in Supplementary Information).

A

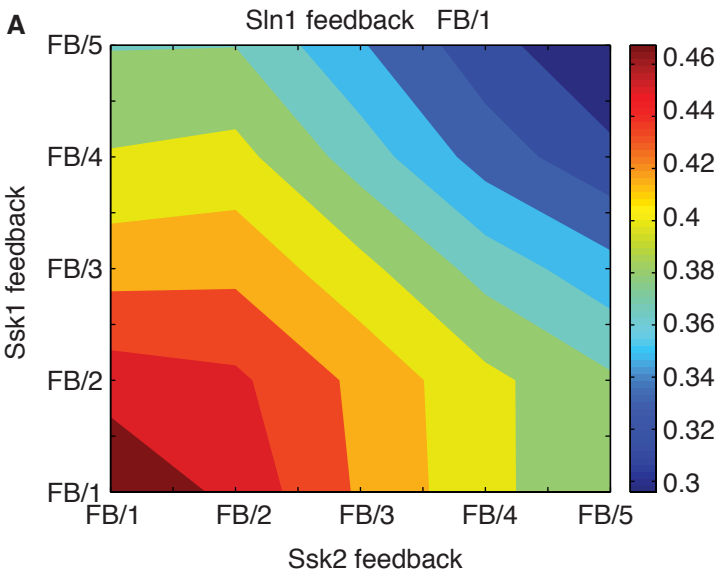
Sln1 feedback FB/1
FB/5
FB/4
FB/3
FB/2
FB/1
Ssk1 feedback
FB/1
FB/2
FB/3
FB/4
FB/5
Ssk2 feedback
0.46
0.44
0.42
0.4
0.38
0.36
0.34
0.32
0.3

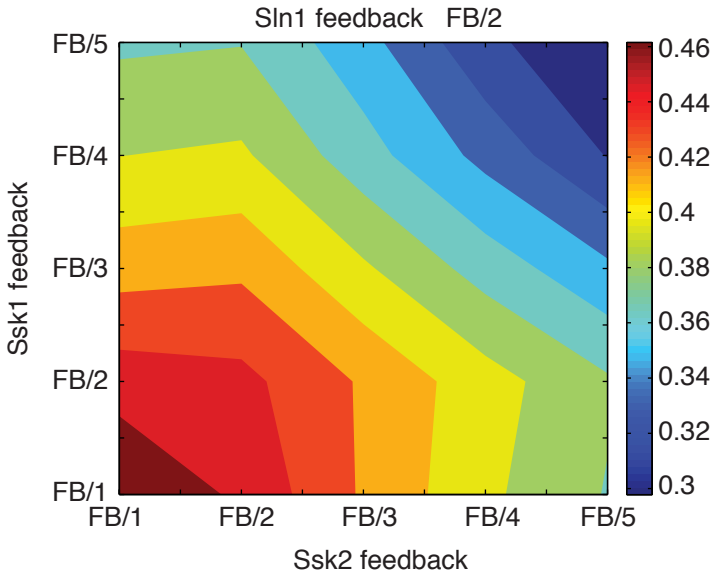
Sln1 feedback FB/2
FB/5
FB/4
FB/3
FB/2
FB/1
Ssk1 feedback
FB/1
FB/2
FB/3
FB/4
FB/5
Ssk2 feedback
0.46
0.44
0.42
0.4
0.38
0.36
0.34
0.32
0.3

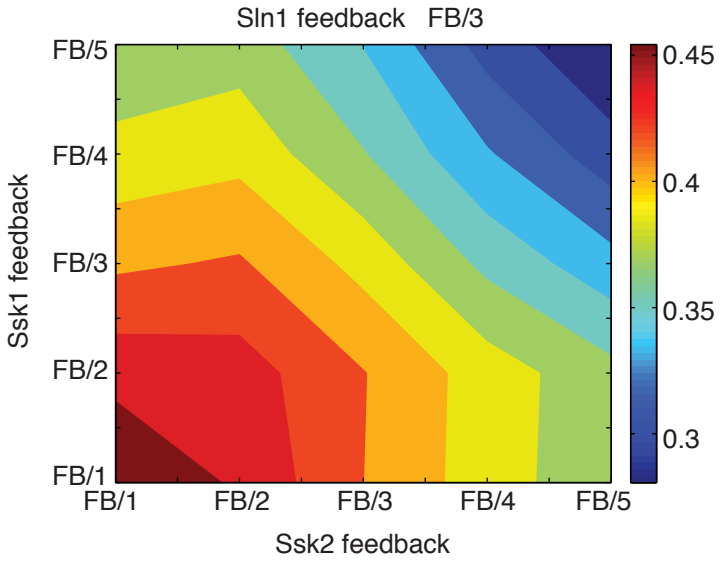
Sln1 feedback FB/3
FB/5
FB/4
FB/3
FB/2
FB/1
Ssk1 feedback
FB/1
FB/2
FB/3
FB/4
FB/5
Ssk2 feedback
0.45
0.4
0.35
0.3

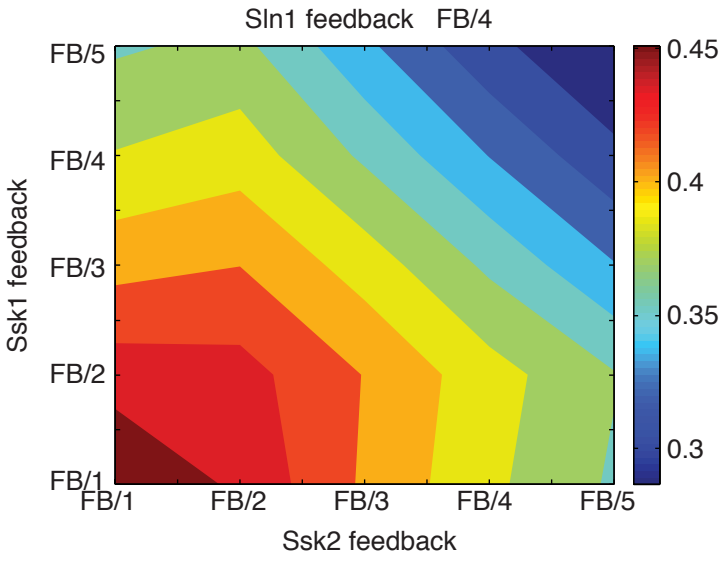
Sln1 feedback FB/4
FB/5
FB/4
FB/3
FB/2
FB/1
Ssk1 feedback
FB/1
FB/2
FB/3
FB/4
FB/5
Ssk2 feedback
0.45
0.4
0.35
0.3

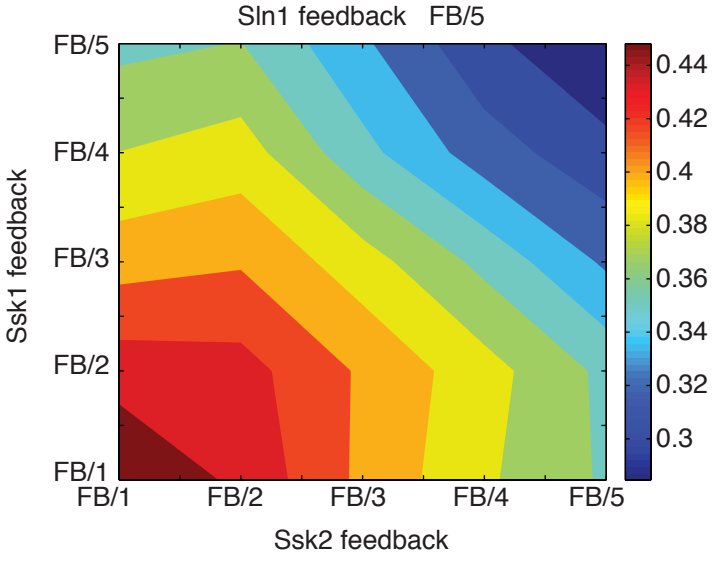
Sln1 feedback FB/5
FB/5
FB/4
FB/3
FB/2
FB/1
Ssk1 feedback
FB/1
FB/2
FB/3
FB/4
FB/5
Ssk2 feedback
0.44
0.42
0.4
0.38
0.36
0.34
0.32
0.3

B

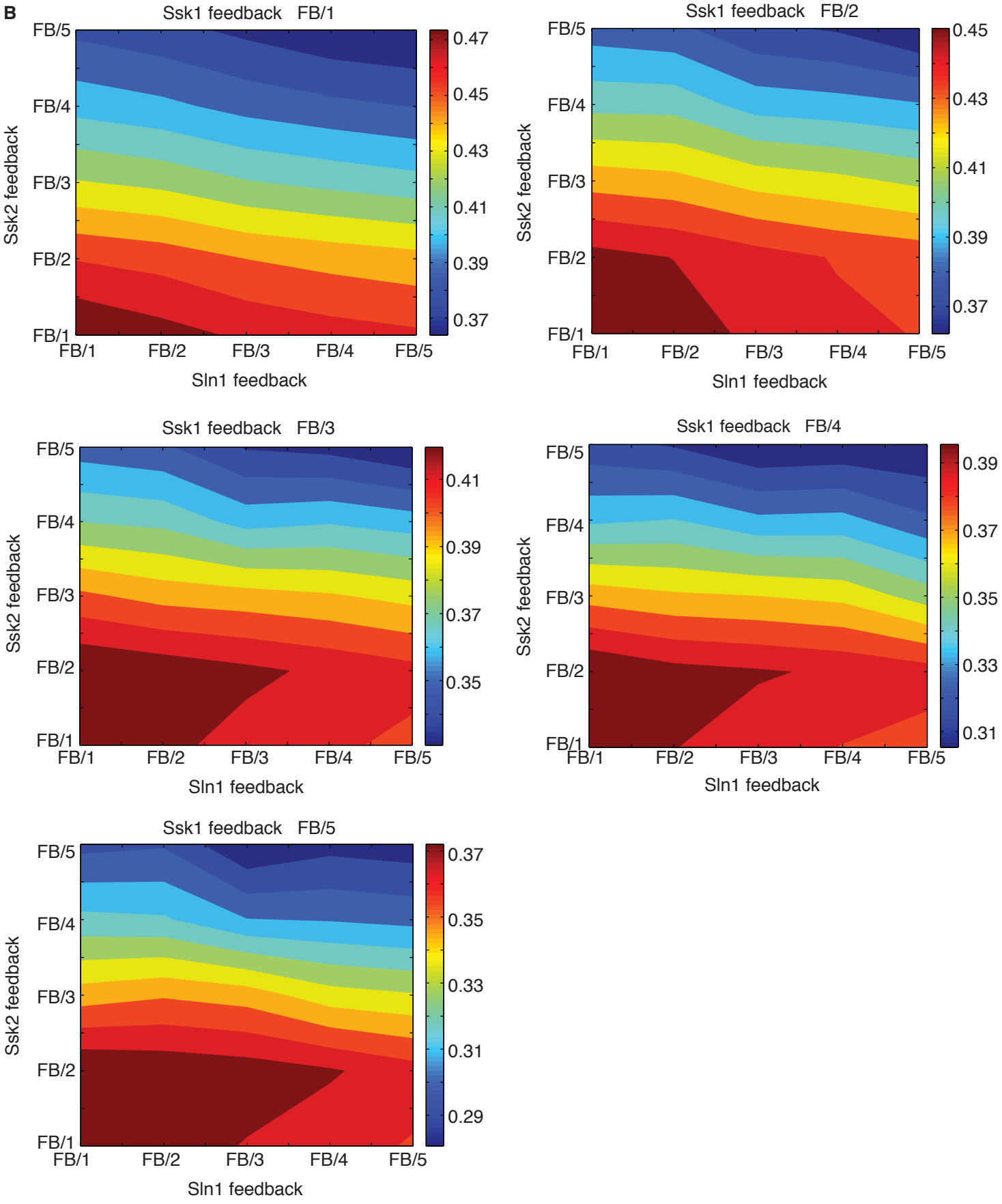
Ssk1 feedback FB/1
Ssk1 feedback FB/2
Ssk1 feedback FB/3
Ssk1 feedback FB/4
Ssk1 feedback FB/5
Ssk2 feedback
Sln1 feedback
FB/1
FB/2
FB/3
FB/4
FB/5
0.47
0.45
0.43
0.41
0.39
0.37
0.35
0.33
0.31
0.29

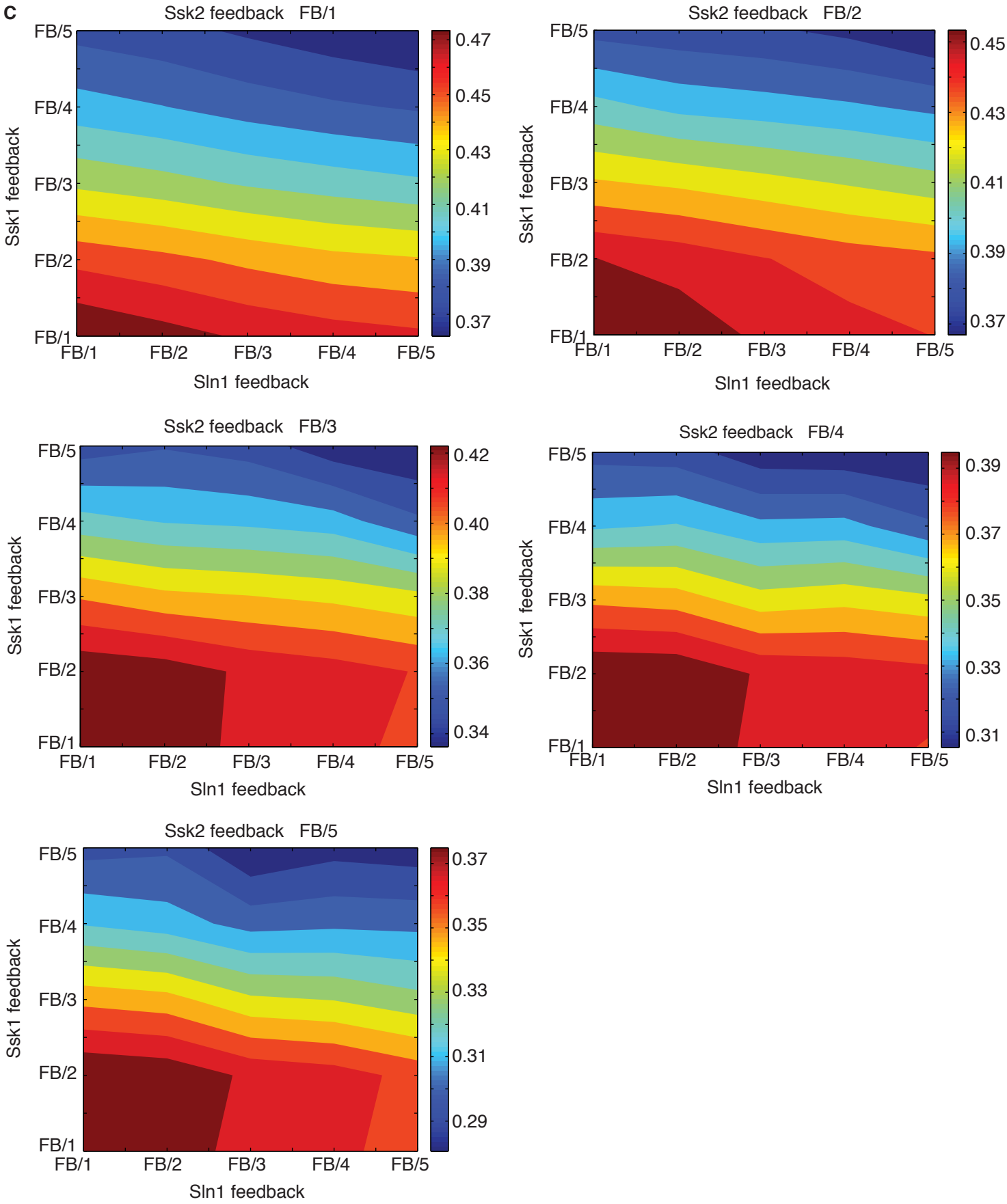

Fig. S 11: Effect of the parameters variations on the signaling feedback efficiency (SFE)
A-C The feedback parameters [k1, k_1, k2, kp] (binding, dissociation, release and dephosphorylation rates) for the three feedback loops were varied simultaneously. FB/n is the feedback parameters divided by n. The SFE is calculated for 125 different sets of parameters, and colors represent the value of SFE for one set of parameters. Note that the SFE shows little change with varying Sln1 feedback parameters.

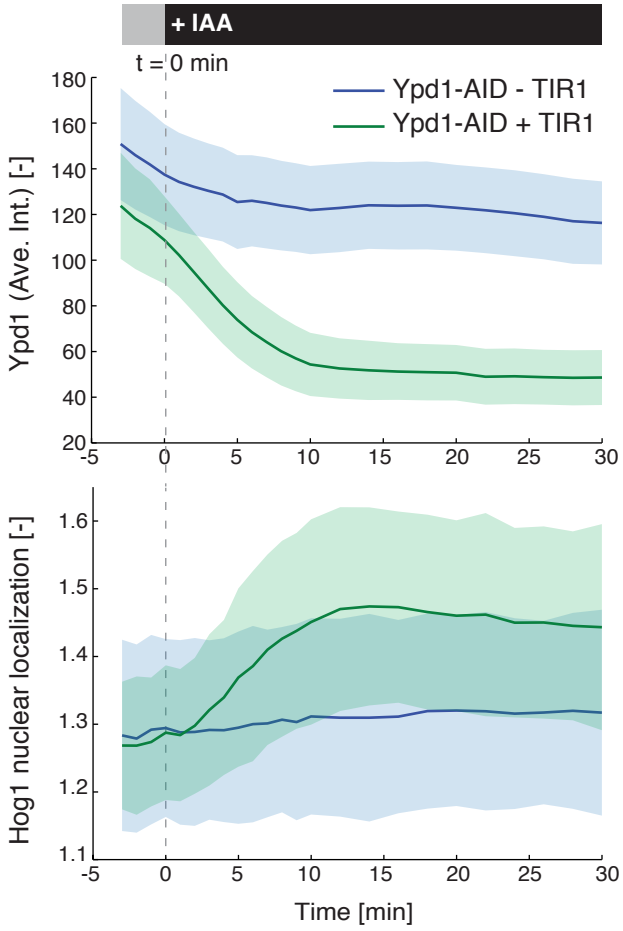

Fig. S 12: Auxin induced Ypd1 degradation using the AID system results in Hog1 activity. Ypd1-GFP fused to the “AID” degron was integrated in cells containing (+ TIR1, green, n=403) or not (- TIR1, blue, n=557) the F-box protein TIR1. Ypd1-GFP degradation was followed by imaging a time series after addition of 500μM IAA at time 0 in which the GFP signal was quantified (upper graph). To avoid crosstalk between Hta2-CFP and Ypd1-GFP signals, Ypd1-GFP was imaged using the YFP filter. Hog1-mCherry activation as a result of Ypd1 degradation was monitored by measuring its nuclear translocation (lower graph).

A

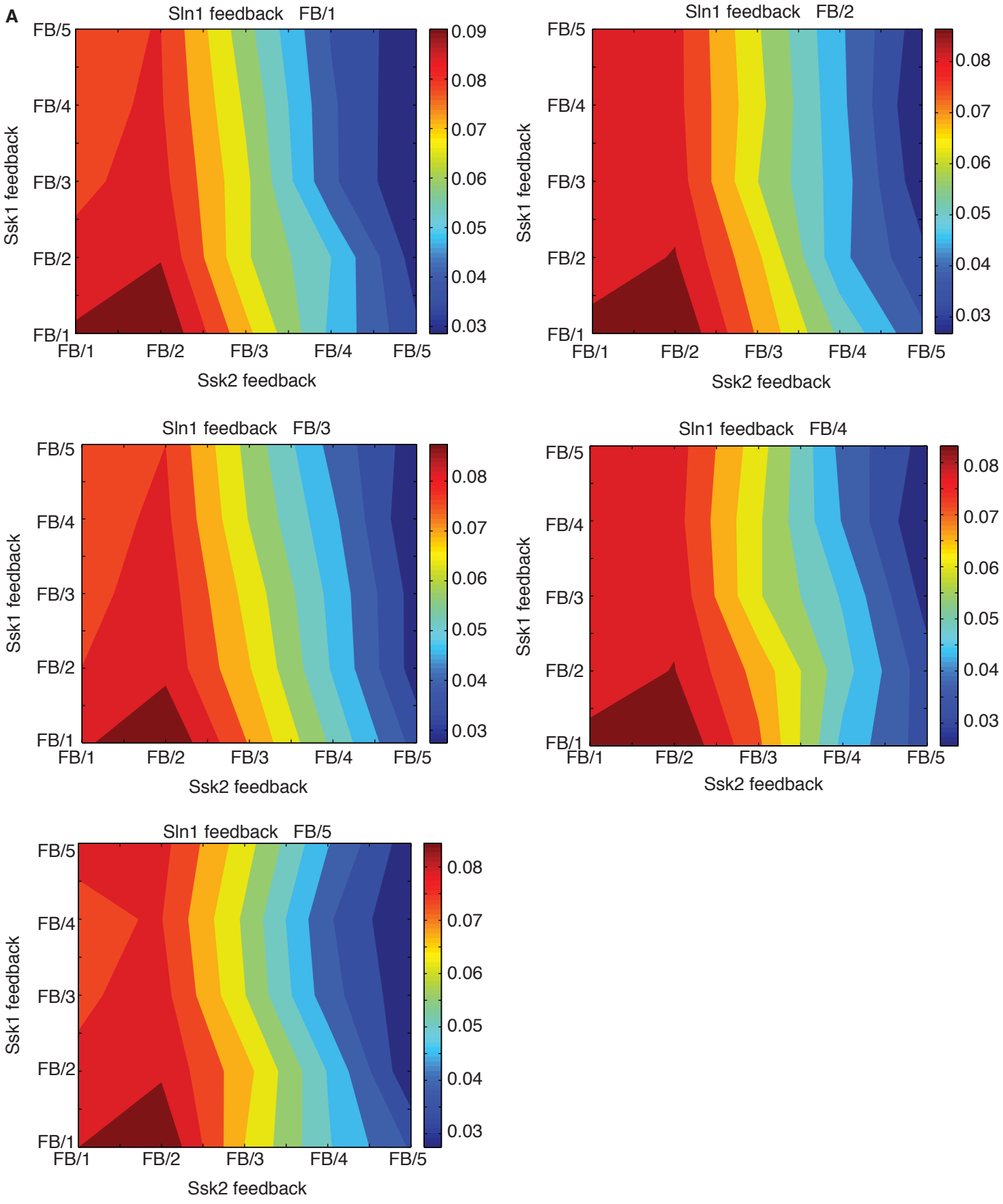
Sln1 feedback FB/1
Sln1 feedback FB/2
Sln1 feedback FB/3
Sln1 feedback FB/4
Sln1 feedback FB/5
Ssk1 feedback
Ssk2 feedback
FB/1
FB/2
FB/3
FB/4
FB/5
0.09
0.08
0.07
0.06
0.05
0.04
0.03

B

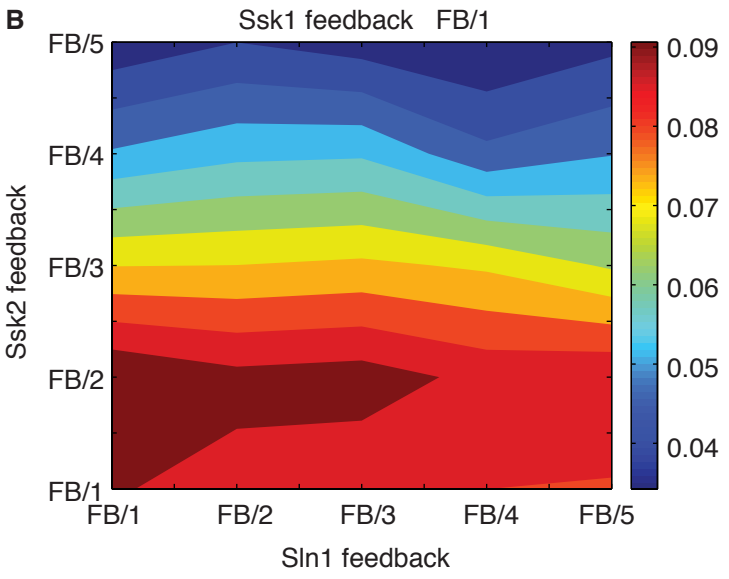
Ssk1 feedback FB/1
FB/5
FB/4
FB/3
FB/2
FB/1
Ssk2 feedback
FB/1
FB/2
FB/3
FB/4
FB/5
Sln1 feedback
0.09
0.08
0.07
0.06
0.05
0.04

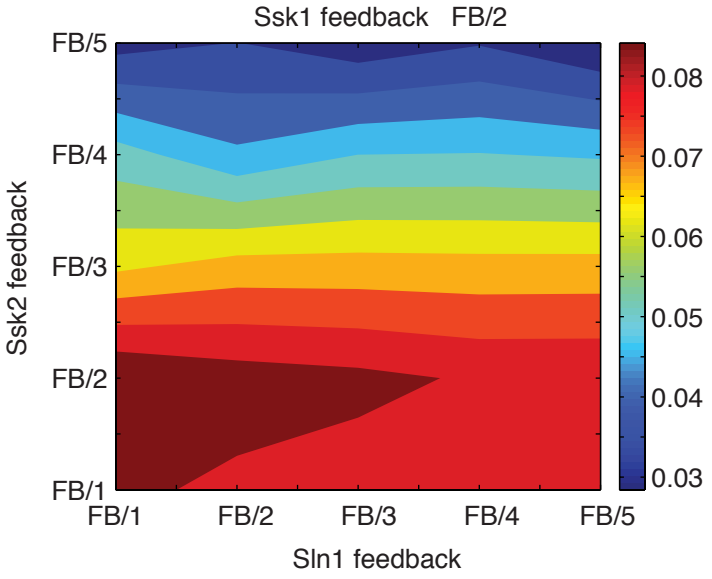
Ssk1 feedback FB/2
FB/5
FB/4
FB/3
FB/2
FB/1
Ssk2 feedback
FB/1
FB/2
FB/3
FB/4
FB/5
Sln1 feedback
0.08
0.07
0.06
0.05
0.04
0.03

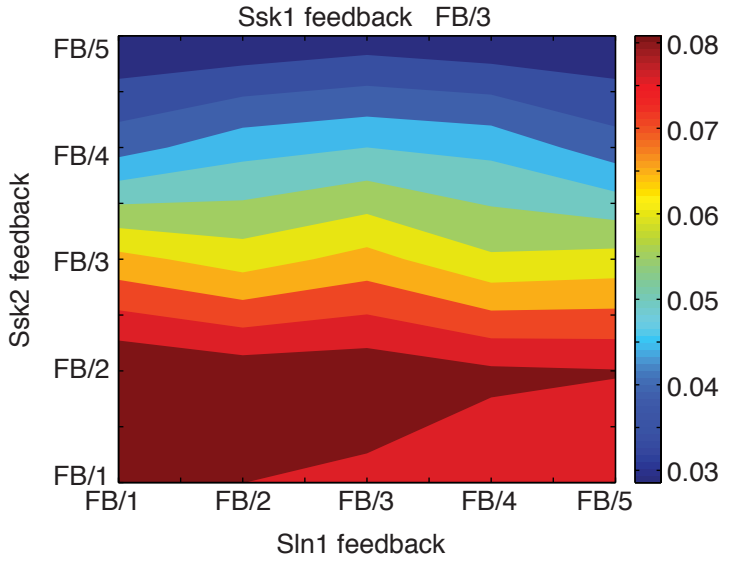
Ssk1 feedback FB/3
FB/5
FB/4
FB/3
FB/2
FB/1
Ssk2 feedback
FB/1
FB/2
FB/3
FB/4
FB/5
Sln1 feedback
0.08
0.07
0.06
0.05
0.04
0.03

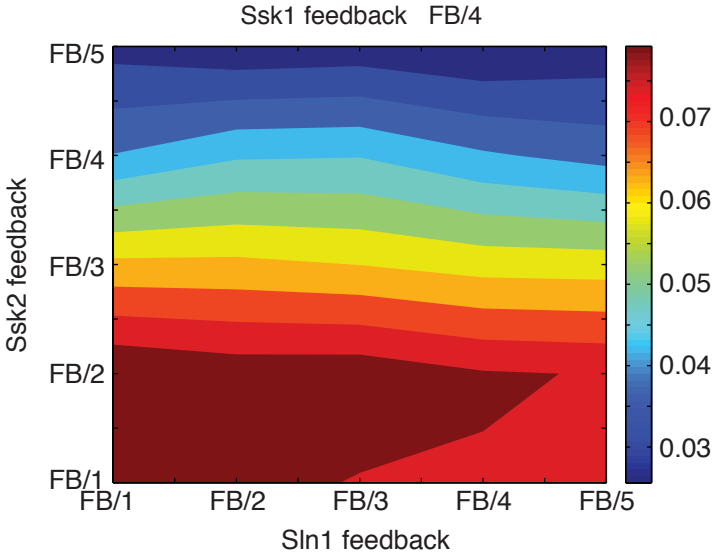
Ssk1 feedback FB/4
FB/5
FB/4
FB/3
FB/2
FB/1
Ssk2 feedback
FB/1
FB/2
FB/3
FB/4
FB/5
Sln1 feedback
0.07
0.06
0.05
0.04
0.03

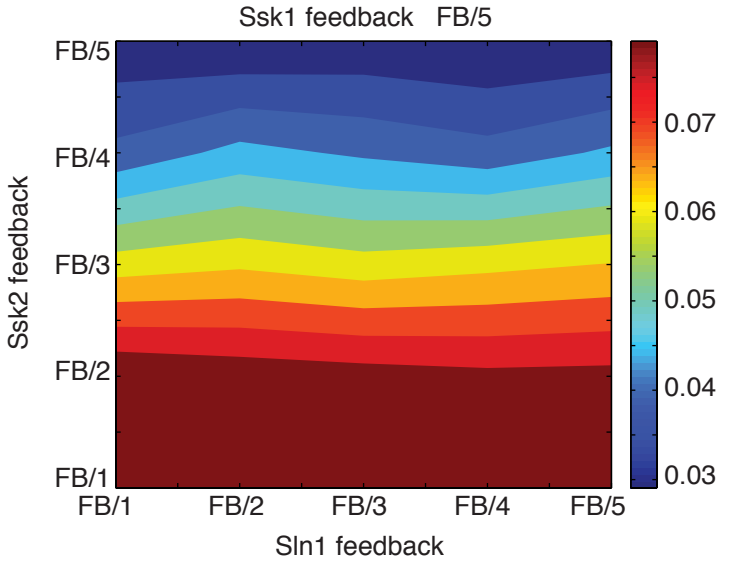
Ssk1 feedback FB/5
FB/5
FB/4
FB/3
FB/2
FB/1
Ssk2 feedback
FB/1
FB/2
FB/3
FB/4
FB/5
Sln1 feedback
0.07
0.06
0.05
0.04
0.03

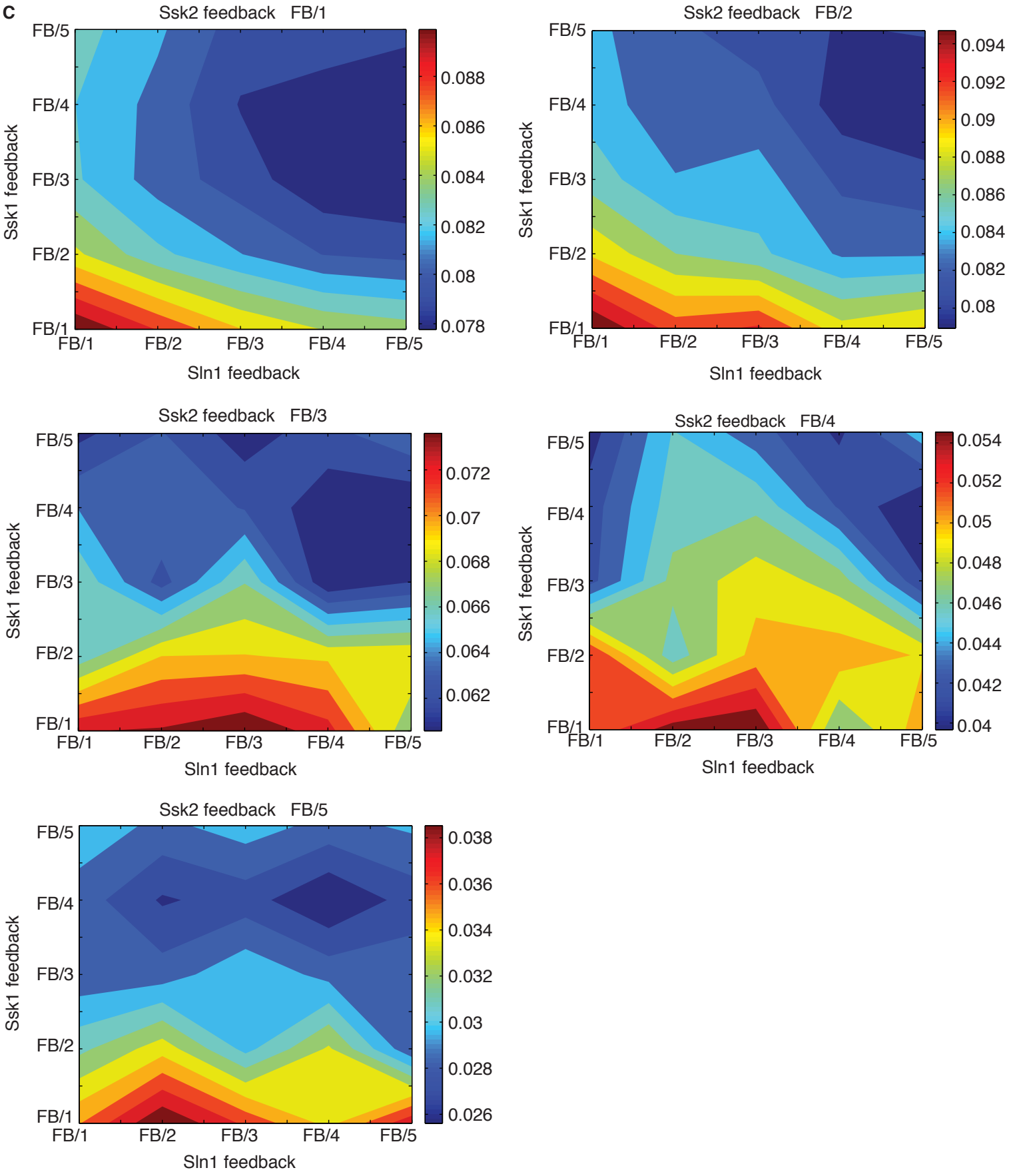

Fig. S 13: Effect of the parameters variations on the signaling feedback efficiency (SFE) when Ypd1 was degraded.s

A-C The model was simulated for the case that Ypd1 was degraded. SFE was calculated for 125 sets of parameters as described in Fig S11. The SFE is only weakly sensitive to Ssk1 and Sln1 feedback parameters and only changes upon varying the feedback strength of Ssk2.

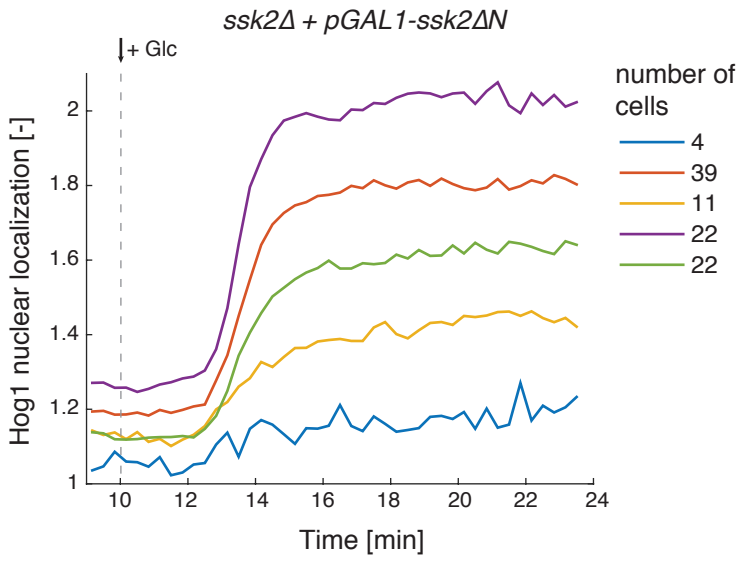

Fig. S 14: Hog1-mCherry cells show comparable nuclear translocation dynamics irrespective of the varying *ssk2ΔN* levels.

Hog1 nuclear localization was quantified upon addition of glucose in *ssk2Δ* cells expressing *ssk2ΔN* from the β-estradiol-inducible promoter. Single cell traces were clustered in 5 classes using the whole time course data and the Squared Euclidian distance method.

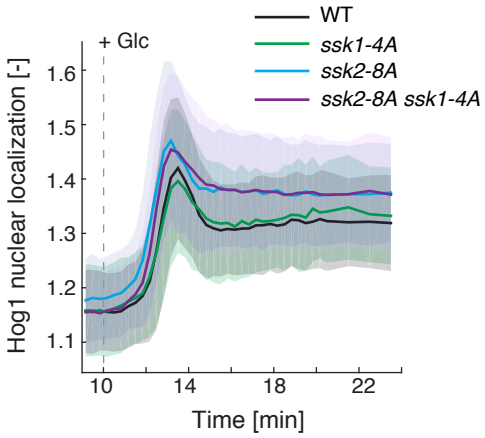

Fig. S 15: Experimental data showing Hog1 nuclear localization over time from images processed as in Fig. 1G of wild-type (WT, black, n=314), *ssk1-4A* (green, n=222) where S110, S193, S195 and S351 are mutated to alanine, *ssk2-8A* (blue, n=380) and *ssk2-8Assk1-4A* cells (purple, n=287). The mutants were integrated in the deletion backgrounds with their endogenous promoters. The glucose-switch was implemented as in Fig 2C. The shaded areas show the standard deviation of the averaged data from indicated number of cells.